Thermodynamic Regulation of Human Short-Chain Acyl-CoA Dehydrogenase by Substrate and Product Binding†

Amy K. Saenger,‡ Tien V. Nguyen,§ Jerry Vockley,§,⊥ and Marian T. Stankovich*,‡

Department of Chemistry, University of Minnesota, 207 Pleasant Street, SE Kolthoff and Smith Halls, Minneapolis, Minnesota 55455 and Department of Medical Genetics, Mayo Clinic and Foundation, Rochester, Minnesota 55905

Received June 2, 2005; Revised Manuscript Received September 15, 2005

ABSTRACT: Human short-chain acyl-CoA dehydrogenase (hSCAD) catalyzes the first matrix step in the mitochondrial β-oxidation cycle for substrates with four and six carbons. Previous studies have shown that the act of substrate/product binding induces a large enzyme potential shift in acyl-CoA dehydrogenases. The objective of this work was to examine the thermodynamic regulation of this process through direct characterization of the electrochemical properties of hSCAD using spectroelectrochemical methodology. A large amount of substrate activation was observed in the enzymatic reaction of hSCAD (+33 mV), the greatest magnitude measured in any acyl-CoA dehydrogenase to date. To examine the role of the substrate as well as the product in electron transfer by hSCAD, a catalytic base mutation (E368Q) was constructed. The E368Q mutation inactivates the reductive and oxidative pathways such that the individual effects of substrate and product binding on the redox potential can be investigated. Optimal substrate (butyryl-CoA) was seen to shift the flavin redox potential slightly more positive (+38 mV) than did optimal product (crotonyl-CoA) (+31 mV), a finding opposite of that observed in another short-chain enzyme, bacterial SCAD. These results indicate that substrate redox activation occurs in hSCAD leading to a large enzyme midpoint potential shift. Substrate binding in hSCAD appears to make a larger contribution than does product to thermodynamic modulation.

Mammalian short-chain acyl-coenzyme A dehydrogenase (SCAD)[1] catalyzes the first step of the β-oxidation cycle, providing up to 40% of the total human energy requirement (*1*). In this reaction, a saturated straight-chain fatty acyl-CoA thioester is converted to an α,β-*trans*-enoyl-CoA thioester via a reversible, asymmetrically concerted abstraction of the α-proton by the catalytic base (Glu368 in human SCAD, Glu367 in bacterial SCAD) and transfer of the β-hydride to the enzyme bound flavin. The reduced acyl-CoA dehydrogenase (ACD) then transfers its electrons to an electron transferring flavoprotein and ultimately to the electron transport chain. Electron transfer from the substrate to the flavin cofactor appears to be thermodynamically forbidden, yet electrochemical and spectroscopic studies have shown that favorable thermodynamic conditions for substrate turnover exist only in the presence of enzyme bound substrate/product (*2*). A positive shift in the reduction potential of the enzyme upon substrate/product binding allows isopotential electron transfer to occur. These findings suggest that the enzyme is regulated by substrate binding. While the mechanism of regulation has not totally been elucidated, it has been shown that upon ligand binding, the active site of the enzyme becomes desolvated and two hydrogen bonds form to the thioester carbonyl of the acyl-CoA (*3*). Use of product analogues has also led to the conclusion that the act of binding itself induces polarization in the ligand (*4*−*6*).

A large body of literature exists on the enzyme mechanism of pig medium-chain acyl-CoA dehydrogenase (pMCAD) and bacterial short-chain acyl-CoA dehydrogenase (bSCAD) enzymes. Although these two enzymes are extremely similar in their biological and molecular properties, there are differences in their redox properties (*2*, *6*), optimal substrate chain length specificities, direction of electron transfer (in vivo), and polarization of transition-state product analogues (*7*). Human SCAD (hSCAD) has been cloned and over-expressed and appears to have similar properties to both pMCAD and bSCAD.

Substrate turnover in ACDs makes it difficult to directly distinguish the effects of substrate and product binding separately and to examine each ligand's contribution to thermodynamic regulation of the enzyme. In previous studies

† This work was supported by grants from the National Institutes of Health (GM29344) to MTS and (GM08700-03) to A.K.S. J.V. was supported in part by PHS Grant RO1-DK54936 from the NIDDK and by the Pennsylvania Department of Health Tobacco Formula Funding.

* To whom correspondence should be addressed. Address: 207 Pleasant St. SE, Minneapolis, MN 55455. Phone: (612) 624-1019. Fax: (612) 626−7541. E-mail: stankovi@chem.umn.edu.

‡ University of Minnesota.

§ Mayo Clinic and Foundation.

⊥ Present address: University of Pittsburgh School of Medicine, Children's Hospital of Pittsburgh, Department of Pediatrics, 3705 5th Avenue, Pittsburgh, PA 15213.

[1] Abbreviations: CoA, coenzyme A; FAD, flavin adenine dinucleotide; ACD, acyl-coenzyme A dehydrogenase; SCAD, short-chain acyl-coenzyme A dehydrogenase; MCAD, medium-chain acyl-coenzyme A dehydrogenase; ETF, electron-transferring flavoprotein; BCoA, butyryl-coenzyme A; CCoA, crotonyl-coenzyme A; K_{dox}, binding constant; E_m, general midpoint potential; $\hat{E}_m$, conditional midpoint potential; $E_{ox/hq}$, midpoint potential for the flavin oxidized/hydroquinone couple; $E_{BCoA/CCoA}$, midpoint potential for the butyryl-coenzyme A/crotonyl-coenzyme A couple; $\hat{E}$, conditional midpoint potential; SHE, standard hydrogen electrode; SDS, sodium dodecyl sulfate.

10.1021/bi051048y CCC: $30.25
Published on Web 11/11/2005

conducted with bSCAD, a catalytic base (E367Q) mutant was constructed to eliminate substrate turnover. Indeed, removal of the hydroxyl group on the catalytic base resulted in a kinetically inactive protein. Results from this study indicated a positive redox potential shift (E_m) when the enzyme is product (crotonyl-CoA) bound (+30 mV) but a negative potential shift when it is substrate (butyryl-CoA) bound (−9 mV) (*8*). It was determined that product binding makes significant contributions to enzyme activation in bSCAD. However, because bSCAD catalyzes the opposite reaction in vivo compared to mammalian ACDs, it is unclear whether these potential shifts are due to physiological differences between the enzymes or if the redox shifts experimentally determined are actually due to product binding. To probe these differences further, an E368Q hSCAD mutant, functionally equivalent to the E367Q bSCAD mutation, was constructed and its properties were compared to studies conducted with the equivalent bSCAD mutant. Comparison of the enzymes from these two species will aid in the overall insight gained from regulation in a human system.

MATERIALS AND METHODS

Protein Purification. Transformed *Escherichia coli* strain XL1 Blue grown in LB media at 37 °C was produced in large quantities by the Biological Process Technology Institute (BPTI) at the University of Minnesota and frozen at −80 °C. Approximately 50 g of cell paste was allowed to thaw over ice in 50 mM potassium phosphate (KP_i) (pH 7.4) buffer, at which time lysozyme and FAD were added and the mixture was allowed to become homogeneous. The cells were then sonicated and centrifuged, and the supernatant was applied to a diethylaminoethyl-Sepharose (DEAE) column preequilibrated with 50 mM KP_i (pH 7.4), 1 mM EDTA. The protein was washed with the KP_i buffer and eluted using a KCl gradient (0−1 M). The yellow fractions were collected, salted out with ammonium sulfate (45−65%), and applied to a 20 μM ceramic hydroxyapatite FPLC column (BioRad; Hercules, CA). Fractions were eluted using a 5−250 mM KP_i, pH 6.8 gradient. The A280/450 ratio of the enzyme was 4.5, indicating sufficient flavin binding. The final peak fractions were pooled and dialyzed against 50 mM KP_i (pH 7.6) for storage at −80 °C with 20% glycerol until use.

Purification of E368Q hSCAD followed this procedure except for initial cell growth. Expression was performed using the isopropylthio-β-D-galactoside (IPTG) inducible vector pKK223-3 (Pharmacia; Uppsala, Sweden) coexpressed with chaperonins GroEL/GroES in a separate vector as previously described (*9*). Terrific broth containing ampicillin (final concentration: 80 μg/mL) and chloramphenicol (final concentration: 35 μg/mL) was inoculated with bacteria containing these plasmids and allowed to grow overnight at 37 °C with vigorous shaking. The following morning the overnight cultures were added to each of four flasks containing 1 L of Terrific broth with 80 μg/mL of ampicillin and 35 μg/mL of chloramphenicol. The flasks were incubated at 37 °C with shaking until an $OD_{600} = \sim 1.0$ was achieved. IPTG was then added to a final concentration of 0.5 mM, and the cultures were then harvested after 4 h of induction. The cell pellet was washed with cold 50 mM KP_i buffer (pH 7.4) and allowed to stir at room temperature for 20 min after addition of FAD and lysozyme. This cell solution was then sonicated at 385 W and cleared by centrifugation, and the mutant SCAD was purified as above. Concentration of the protein was calculated using the extinction coefficient determined for hSCAD (14.5 ± 0.2 mM^{-1} cm^{-1}) using the method of Williamson and Engle (*10*).

The E367Q mutant bSCAD protein was expressed from *E. coli* strain K19 and grown in Terrific broth to stationary phase at 37 °C with no induction as described by Becker et al. (*11*). A 100 mM, pH 7.0 KP_i buffer was utilized for all studies of bSCAD presented in this work. The concentration of the E367Q bSCAD solution was determined using an extinction coefficient of 13.9 mM^{-1} cm^{-1} at 453 nm (*8*). Activity assays of purified wild-type and mutant hSCAD and bSCAD were performed using the ferricenium assay developed by Lehman and Thorpe (*12*). Sodium dodecyl sulfate−polyacrylamide gel electrophoresis (SDS−PAGE) was used to determine the purity of all enzymes, and all experiments utilized enzyme of greater than 95% purity at 25 °C. ACDs produced in bacterial systems typically exhibit a bright green color indicative of being CoA-persulfide bound. Removal of the CoASH was achieved through the use of a thiopropyl-Sepharose column.

Ligand Preparation and Synthesis. Commercially available substrates and products (butyryl-, crotonyl-, hexanoyl-, and octanoyl-CoA) were obtained from Sigma Chemical Company (St. Louis, MO). These substrates and products were dissolved in glass distilled water prior to use and stored at −20 °C. Valeryl-, pentenoyl-, hexenoyl-, and octenoyl-CoA ligands were synthesized using the mixed anhydride method developed by Bernert et al. (*13*). A total of 40 mg of the commercially available carboxylic acid was weighed and reacted anhydrously in tetrahydrofuran (THF). Triethylamine and isobutylchloroformate were added to react with the acid to make the acid anhydride and the reaction proceeded under an argon atmosphere. The lithium salt of coenzyme A isolated from *E. coli* (LiSCoA) dissolved in a sodium bicarbonate solution (250 mM in water) was added to the acid anhydride mixture to yield the desired thioester. This reaction was allowed to stir overnight under bubbling argon. The pH of the solution was adjusted to 5.0 using glacial acetic acid to quench the reaction.

The solvent was then removed through rotary evaporation, and the residual compound was dissolved in approximately 40 mL of water. The mixture was extracted with diethyl ether to remove any excess unreacted acid, and the aqueous phase extractions were pooled and evaporated under reduced pressure until the volume was less than 1 mL. The resulting residue was redissolved in water and loaded onto a pre-equilibrated C-18 sep-pak (Waters Corporation). Salts and other contaminants were washed off the cartridge with water, and the thioester was eluted with methanol. The methanol was removed by evaporation under reduced pressure until the solution was reduced to approximately 500 μL. In the final purification step, HPLC was performed using a semi-preparative column (C-18, 10.8 mm ID × 25 cm) under the following solvent program: 90% water/10% methanol for 25 min at 0.5 mL/min, followed by a 20 min gradient to 100% methanol, and returning to the original ratio over a 30 min gradient. An online UV detector was used to detect the purified fractions, and spectrophotometric data was used as confirmation of the thioester purity. The fractions were then pooled, evaporated under reduced pressure, and lyo-

philized. Concentrations of all ligands were measured spectrophotometrically using $\epsilon_{260} = 16.0\ mM^{-1}\ cm^{-1}$ for substrates and $\epsilon_{260} = 22.6\ mM^{-1}\ cm^{-1}$ for products (*14*). ^1H NMR was used as an additional method to confirm the purity and composition of the substrates and products.

Binding Constants. Dissociation constants (K_{dox}) for the complex of oxidized enzyme with the ligand of interest were measured and calculated. To determine K_{dox}, a ligand was aerobically titrated into a solution of enzyme. Each aliquot of titrant was added via a modified syringe to the enzyme, which was contained in a 1 mL quartz cuvette. After each addition of ligand, the mixture was briefly mixed, and the absorbance spectrum from 225 to 850 nm of the enzyme−ligand complex was recorded. Changes in the active site of the protein are manifested as a bathochromic shift of the max peak (at 450 nm) and as a shoulder that increases at approximately 485 nm. Changes in absorbance (ΔA) at ca. 485 nm versus the amount of ligand added ([L] in μM) were fitted to a curve using the GraphPad Prism program (eq 1):

$$\Delta A = \frac{\Delta A_{max}}{2[ET]}[(([L] + [ET] + K_d) - (([L] + [ET] + K_d)^2 - \sqrt{(4[ET][L])})] \quad (1)$$

where ΔA_{max} is the calculated maximal absorbance change, $[E_T]$ is the concentration of enzyme used, [L] is the concentration of ligand added, and K_d is the calculated dissociation constant of the oxidized enzyme−ligand complex.

Spectroelectrochemical Methods. Coulometric and potentiometric titrations were essentially performed as described previously (*6*, *15*). All electrochemical experiments performed with hSCAD were conducted in 50 mM KP_i (pH 7.6), while studies with bSCAD were all in 100 mM KP_i (pH 7.0). For coulometric reductive titrations, a concentration of 10−20 μM protein in potassium phosphate buffer was used with 0.1 mM methyl viologen added as a mediator dye to facilitate reduction of the enzyme.

Potentiometric titrations were performed to determine the midpoint potentials of the uncomplexed enzymes, as well as the potential when complexed to a ligand. These experiments were conducted under similar conditions as coulometric titrations, but several indicator dyes (2−5 μM) were added in addition to the methyl viologen: indigo disulfonate ($E_m = -118$ mV, pH 7.6; $E_m = -102$ mV, pH 7.0), pyocyanine ($E_m = -19$ mV, pH 7.6; $E_m = -18$ mV, pH 7.0), and 8-chlororiboflavin ($E_m = -162$ mV, pH 7.6). Indicator dyes were used to facilitate equilibration between the enzyme and the gold working electrode. Electrochemical equilibration typically took between 1 and 3 h per point and was defined as a potential change of <1 mV/10 min. All redox potential values are reported versus a standard hydrogen electrode (SHE).

To determine the midpoint potential of hSCAD in the presence of several substrate/product couples (butyryl-CoA/crotonyl-CoA, valeryl/pentenoyl-CoA, or hexanoyl/hexenoyl-CoA) experiments were performed as previously described by Stankovich et al. (*6*). The spectroelectrochemical cuvette contained approximately 15 μM enzyme, 100 μM methyl viologen, 2 μM indigo disulfonate, and 5 μM pyocyanine in 50 mM KP_i buffer (pH 7.6). In the sidearm of the cell resided a 100 μL solution of the C4, C5, or C6 substrate/product couple. Once the contents of the cell were degassed, the enzymes and the dyes were electrochemically reduced and the equilibrium potential was poised. The substrate/product couple solution was then tipped into the glass cuvette, and the final concentration of the couple was approximately 150 μM each, with a final protein concentration of approximately 10−12 μM. A 10-fold excess of substrate and product ensured that the measured potential was that of the system, equilibrating near the potential of the free, unbound couple (−40 mV) (*2*). The system achieved equilibration after approximately 1 h, at which time the potential of the system was recorded and the visible spectra was obtained.

Anaerobic Substrate Titrations of Wild-Type hSCAD. Wild-type hSCAD protein was titrated with butyryl-, valeryl-, and hexanoyl-CoA substrates as described previously (*6*). Approximately 12−15 μM of hSCAD enzyme in 50 mM KP_i (pH 7.6) was degassed in the glass cuvette of the spectroelectrochemical cell. To remove any residual oxygen prior to the beginning of the experiment, the system was electrochemically reduced using methyl viologen as the mediator dye. A gastight syringe (Hamilton Company; Reno, NV) was used to deliver aliquots of the anaerobic substrate (1.5−5 mM) to the enzyme solution through a syringe port in the electrochemical cell. After each addition of substrate, spectral changes occurred within the system after a maximum time of 10 min, at which point the visible spectra was obtained.

Equipment. UV/Vis spectroscopic measurements were performed using a Perkin-Elmer Lambda 12 spectrophotometer interfaced to an IBM-compatible computer. The Perkin-Elmer Computerized Spectroscopy Software (PECSS) program was used for spectral acquisition and data manipulation. The spectrophotometer was equipped with a thermostated cell to ensure a constant temperature throughout the experiment, and a magnetic stirrer was used to facilitate equilibration of the system. All electrochemical experiments performed were conducted at 25 °C under anaerobic conditions. To achieve optimal anaerobicity, an argon gas line equipped with two different oxygen scrubbers, Riddox and Oxyclear (Fisher Scientific) were used. A BAS-50CV (Bioanalytical Systems) electrochemical analyzer was used to add charge and measure potentials in the spectroelectrochemical experiments.

Calculations. After collection of the electrochemical data, the spectra were corrected for dyes and turbidity and only corrected spectra were used in all calculations. In coulometric experiments the number of electrons transferred during the reaction (n) can be determined based on the number of moles of enzyme being reduced in the sample (eq 2):

$$n = \frac{Q}{NF} \quad (2)$$

where N is the number of moles of material being reduced, Q is the total number of coulombs added (C), and F is Faraday's constant (96485 C/mol). After calculation of n in various points in the experiment, a plot of absorbance vs n was constructed, and the number of electrons transferred in the half-reaction were then determined from the beginning and the end of the titration. An increase in absorbance at 610 nm signals the titration endpoint, due to the stabilization of reduced methyl viologen.

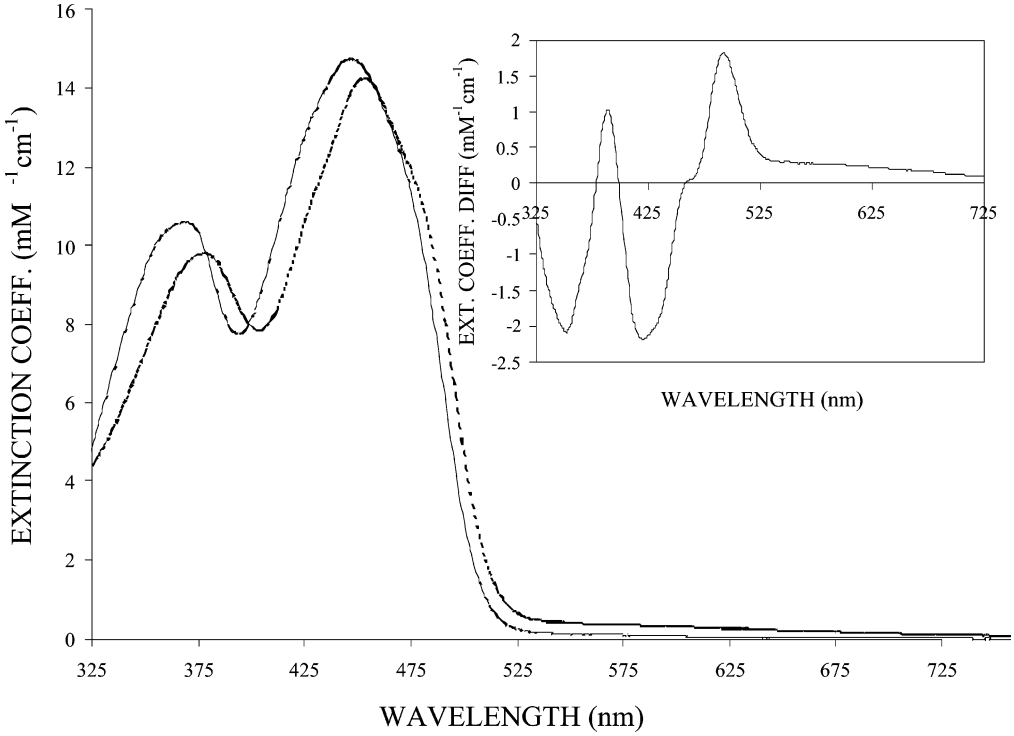

FIGURE 1: Optical spectra of wild-type hSCAD (—) and E368Q hSCAD (- - -). Inset: Extinction coefficient difference between the two enzymes.

The Nernst equation (eq 3) was used to analyze the potentiometric data:

$$E = E_m + 2.303\frac{RT}{nF}\log\frac{[\text{oxidized}]}{[\text{reduced}]} \quad (3)$$

where E is the measured potential of each point at equilibrium, E_m is the midpoint potential, R is the gas constant (8.3145 J mol^{-1} K^{-1}), T is the temperature in degrees Kelvin, n is the number of electrons involved in the half-reaction, and F is Faraday's constant. All midpoint potential determinations were calculated from an average of three trials with a typical error of ± 2−5 mV (*16*). The relationship between individual formal potential values ($E_1^{\circ\prime}$ and $E_2^{\circ\prime}$) and the midpoint potential value used to arrive at the maximal amount of semiquinone thermodynamically stabilized (red anionic or blue neutral) was determined using the equation previously reported by Clark (*17*).

In anaerobic substrate titrations, the conditional potential difference ($\Delta\hat{E}$) is defined as the difference between the midpoint potential for the enzyme complexed with substrate/product and the midpoint potential for the substrate/product couple when enzyme bound. The $\Delta\hat{E}$ can be calculated from eq 4:

$$E_m(SH_2/P \sim EFAD_{ox/red}) = E_m(EFAD_{ox/red} \sim SH_2/P) + 2.303\frac{RT}{nF}\log K_{eq} \quad (4)$$

and is equivalent to eq 5 at the endpoint of the titration:

$$\Delta\hat{E} = \frac{59.2\text{ mV}}{n}\log\frac{[E_{red}]}{[E_{ox}]} \quad (5)$$

The point in the titration when 1 equiv of substrate is equal to 1 equiv of enzyme reflects the internal equilibrium (K_{eq}) between the amount of enzyme complexed with either butyryl-CoA or crotonyl-CoA. The $\Delta\hat{E}$ value is thus determined from the spectra and differs for each titration based upon the amount of flavin reduction observed.

RESULTS AND DISCUSSION

Enzyme Purification and Characterization. All enzymes were purified as intact holoproteins, as judged by their intense yellow color, and showed distinct 44 kDa SDS−polyacrylamide gel bands. The visible spectra of oxidized wild-type hSCAD and E368Q hSCAD are shown in Figure 1. The E367Q bSCAD spectrum is remarkably similar to E368Q hSCAD and thus is not shown (*11*). Calculated extinction coefficients and absorbance maxima for each enzyme are presented in Table 1. The major difference between the wild-type enzyme and the kinetically inactive forms of each enzyme is that a slightly higher resolution and red shift of the 450 nm peak is observed (inset, Figure 1). The UV−CD spectra of the normal and E367Q mutant bSCAD are identical (*11*), and this finding holds true for hSCAD as well (Vockley, unpublished data). This indicates that there are no major global conformational changes that occurred upon mutation of the wild-type enzyme. The UV−visible spectra for all enzymes are also similar; therefore, modifications near the environment of the flavin binding site are minimal.

Incubation of the E368Q hSCAD mutant with an excess amount of butyryl-CoA (BCoA) substrate (30-fold) was performed to test the reductive half-reaction. The flavin spectrum of the protein was recorded at various times during the incubation period (25 °C, pH 7.6). Immediately upon addition of the BCoA, binding of the substrate was evident due to the appearance of a shoulder in the flavin region and a red shift of the 450 nm peak. Incubation was allowed to proceed for 24 h, after which time the amount of bleaching

Table 1: Spectral Properties of Uncomplexed Wild-Type hSCAD and Uncomplexed and Complexed Mutant E368Q hSCAD and E367Q bSCAD

enzyme	ligand	λ_{max} (nm)	ϵ_λ ($mM^{-1}\,cm^{-1}$)
WT	none	448	14.5 ± 0.2
E368Q hSCAD	none	452	14.3 ± 0.4
	butyryl-CoA	456	14.2 ± 0.3
	crotonyl-CoA	454	14.0 ± 0.3
	valeryl-CoA	455	14.4 ± 0.2
	pentenoyl-CoA	455	13.9 ± 0.1
	hexanoyl-CoA	454	14.1 ± 0.2
	hexenoyl-CoA	456	14.1 ± 0.4
	octanoyl-CoA	452	13.8 ± 0.5
	octenoyl-CoA	453	14.0 ± 0.3
E367Q bSCAD	none[a]	453	13.9 ± 0.2
	butyryl-CoA[a]	457	13.4 ± 0.3
	crotonyl-CoA[a]	459	13.5 ± 0.3
	valeryl-CoA	459	13.2 ± 0.1
	pentenoyl-CoA	458	13.3 ± 0.2
	hexanoyl-CoA	457	13.3 ± 0.4
	hexenoyl-CoA	456	13.4 ± 0.5

[a] From ref *8*.

in the flavin spectrum was only 5% of the bleaching observed in a similar experiment with wild-type hSCAD and BCoA (data not shown). Therefore, it was determined that the E368Q mutant would not result in substrate turnover during spectroelectrochemical experiments and would be a good candidate for investigation into substrate modulation of hSCAD. Enzymatic activity assays with ferricenium and pig ETF as electron acceptors demonstrated negligible amounts of activity compared to the wild-type enzyme (<0.05%).

Redox Properties of Uncomplexed Wild-Type hSCAD. The two-electron reduction potential ($E_{ox/hq}$) of wild-type hSCAD was measured at pH 7.6 using established spectroelectrochemical methods (*6*, *15*). Electrochemical studies were performed at this pH due to the stability of the enzyme and to facilitate comparison to other ACD systems previously studied. Coulometric experiments revealed that reduction of the enzyme requires two electrons, and spectral changes occurred at wavelengths less than 550 nm, with a single isosbestic point present at 340 nm. There was a lack of absorbance around 580 nm, indicative of little (<5%) or no blue neutral semiquinone thermodynamic stabilization during both types of electrochemical titrations. A typical potentiometric titration is shown in Figure 2. The Nernst plot (inset, Figure 2) yields an $E_{ox/hq}$ value for the protein (-162 ± 3 mV) and also supports the findings of the coulometric data obtained, with a slope of 29.4. This is close to the theoretical value of 30 mV for a two-electron transfer.

Comparison between wild-type hSCAD and other ACD enzymes such as pMCAD ($E_{ox/hq} = -145$ mV) (*18*), human MCAD (hMCAD) ($E_{ox/hq} = -114$ mV) (*19*), and bSCAD ($E_{ox/hq} = -79$ mV) (*20*) reveals that the midpoint potential of uncomplexed wild-type hSCAD is the most negative, indicating that electron transfer in this enzyme is highly unfavorable. The $E_{ox/hq}$ of human SCAD is 48 mV more negative than that of human MCAD; therefore, it appears that the large degree of regulation proposed to occur in this system is specific to the SCAD enzyme rather than to human ACDs in general. Comparisons of mammalian versus bacterial ACDs and short-chain versus medium-chain ACDs make it clear that a high degree of enzyme regulation is essential for electron transfer in hSCAD to commence.

Midpoint Potentials of Substrate/Product Complexed hSCAD. Substrate/product binding has been determined to be a critical factor in ACD electron transfer, causing a potential shift of up to 120 mV (*2*). When this binding phenomena occurs, the flavin cofactor of the enzyme becomes nearly isopotential with the substrate/product couple and electron-transfer regulation somehow modulated by this binding. Raman and spectroelectrochemical studies have shown that polarization of the product induced through hydrogen-bond interactions is responsible for some of this redox potential shift (*18*, *21*). However, it is unclear how the extent of the positive shift of the FAD cofactor relates to modulation in the enzyme.

To examine the effects of substrate/product binding on the potential shift of the flavin cofactor in wild-type hSCAD, conditional midpoint potentials ($\hat{E}_{ox/hq}$) were determined in the presence of three substrate/product couples present at 10-fold excess concentrations compared to protein: butyryl/crotonyl-CoA (C4), valeryl/pentenoyl-CoA (C5), and hexanoyl/hexenoyl-CoA (C6). Addition of each substrate/product couple resulted in minor changes in the cell potential and various degrees of flavin bleaching. All potential and spectral changes were stabilized after approximately 1 h, at which point the solution was allowed to remain at the poised potential to ensure no further changes were occurring. Typical spectral changes occurring during this type of experiment were similar to those presented elsewhere (*6*, *20*). Charge-transfer bands were evident after addition of each substrate/product couple, characteristic of complexes forming between the reduced flavin and the product.

After subtraction of the indicator dyes from the spectra, the concentrations of each of the enzyme complexes were determined from the absorbance at the flavin maxima (448 nm) and the absorbance at 580 nm. An extinction coefficient for the uncomplexed oxidized wild-type hSCAD was calculated as described earlier ($\epsilon_{448} = 14.5\ mM^{-1}\,cm^{-1}$), and the extinction coefficient for each product bound enzyme was also calculated and found to be slightly lower (crotonyl-CoA bound $\epsilon_{448} = 13.4\ mM^{-1}\,cm^{-1}$; pentenoyl-CoA bound $\epsilon_{448} = 13.1\ mM^{-1}\,cm^{-1}$; hexenoyl-CoA bound $\epsilon_{448} = 12.8\ mM^{-1}\,cm^{-1}$).

Substrate and product are believed to bind tightly to the reduced form of wild-type bSCAD (*6*, *8*). Because of the similarities between hSCAD and bSCAD, similar binding was assumed for the hSCAD enzyme, and therefore there should be no uncomplexed reduced enzyme present at equilibrium. The extinction coefficients used in calculations for the substrate ($\epsilon_{450} = 2.0\ mM^{-1}\,cm^{-1}$) and product ($\epsilon_{450} = 4.0\ mM^{-1}\,cm^{-1}$ and $\epsilon_{580} = 3.0\ mM^{-1}\,cm^{-1}$) bound reduced enzyme were assumed to be the same as the values obtained in earlier stopped-flow studies with mammalian MCAD (*22*).

The calculated values for the $\hat{E}_{ox/hq}$ hSCAD bound to each substrate/product couple is pictorially shown in Figure 3 (unfilled bars). These conditional midpoint potential values were calculated using the Nernst equation and the measured potential of the system at equilibrium. For hSCAD binding to its optimal C4 substrate/product couple, binding caused a +110 mV shift (from −162 to −52 mV), a value that is extremely close to the value obtained from MCAD binding to its optimal C8 substrate/product couple (+120 mV). However, in the MCAD protein this large potential shift is

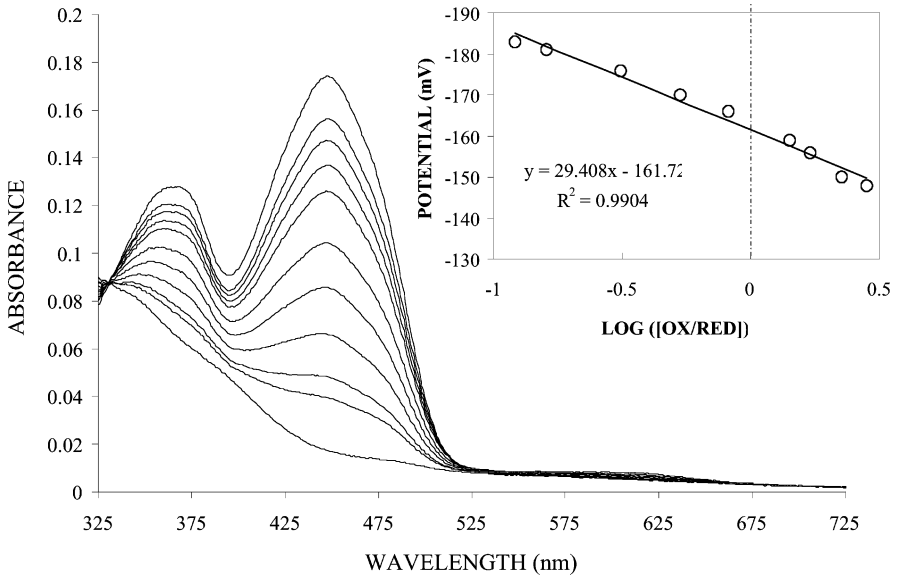

FIGURE 2: Potentiometric titration of uncomplexed wild-type hSCAD. Titration was performed in 50 mM potassium phosphate buffer (pH 7.6) containing 100 μM methyl viologen, indigo disulfonate (2 μM), pyocyanine (5 μM), and 8-chlororiboflavin (2 μM) at 25 °C under anaerobic conditions. Curve 1, fully oxidized spectrum. Curves 2−10; $E = -147$, -149, -155, -158, -165, -169, -175, -180, and -182 mV, respectively. Curve 11, fully reduced spectrum. Inset: Nernst plot indicating $E_m = -162$ mV.

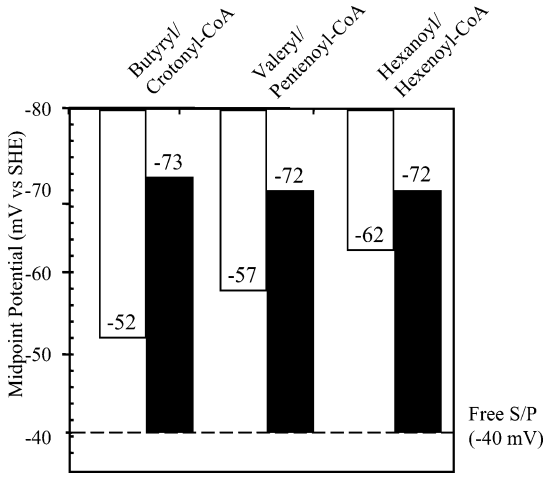

FIGURE 3: Comparison of the thioester substrate/product couples and flavin midpoint potential shifts in the hSCAD•substrate/product complexes. The unfilled bars represent the enzyme potential shift when bound to each specific S/P couple ($\hat{E}_{ox/hq}$). The solid bars show the midpoint potential shift of the S/P couple upon binding to hSCAD.

enough for the enzyme and the substrate/product couple to become isopotential without any other thermodynamic barrier. In hSCAD, there is still a 12 mV (3.0 kcal) barrier to be overcome.

Interestingly, the $\hat{E}_{ox/hq}$ values become more negative upon increasing chain length of the substrate/product couple. With each increasing carbon on the substrate/product couple, the flavin potential shift is 5 mV less. Although this is not a particularly sizable potential change between the thioester couples, it still demonstrates that hSCAD is most finely tuned to its optimal substrate/product couple. Thus, binding of each subsequently longer chain length couple creates a more unfavorable environment for electron transfer to occur and increases the $\Delta G°$ needed to overcome the thermodynamic barrier.

Effect of Binding on the Potential of the Substrate/Product Couple. Binding of the substrate/product couple significantly shifts the redox potential of wild-type hSCAD, yet an energy obstacle remains that needs to be overcome for electron transfer to initiate. To examine the extent of modulation in the actual substrate/product couples themselves, anaerobic substrate titrations were performed using natural thioester substrates (butyryl-, valeryl-, and hexanoyl-CoA). Direct electrochemical measurements of the substrate/product couple cannot be determined because the optical spectra of the substrates and products overlap in the UV region of the spectrum, where there are also large spectral contributions from the protein. To circumvent this, the conditional potential differences ($\Delta\hat{E}$) between the $\hat{E}_{ox/hq}$ value for the bound enzyme and $E_{sub/prod}$ value for the couple can be estimated if the equilibrium constants are known for the electron-transfer reactions. Detailed methodology of calculation of $\Delta\hat{E}$ from spectral data acquired during the substrate titration has previously been reported (*6*, *20*).

Figure 4 illustrates a typical anaerobic substrate titration; shown is the reduction of wild-type hSCAD with butyryl-CoA. After addition of known aliquots of the substrate, various degrees of flavin bleaching are observed as well as an increase in the charge-transfer (CT) band, centered at 580 nm. The CT complex forms between the highest occupied molecular orbital (HOMO) of the flavin and the lowest unoccupied molecular orbital (LUMO) of the polarized substrate/product (*23*, *24*). The inset of Figure 4 also illustrates the simultaneous reduction of flavin and increase of the CT band. The A_{450} plotted against the amount of BCoA added is not linear, suggesting that enzyme reduction is not quantitative and an equilibrium exists among all four species (oxidized and reduced SCAD, and oxidized and reduced substrate) throughout the course of the titration. This equilibrium is consistent with the reductive half-reaction model proposed by Thorpe et al. for MCAD (*25*). We can calculate the potential separation between the two couples from the concentration of the species present at equilibrium using eq 5 (Materials and Methods).

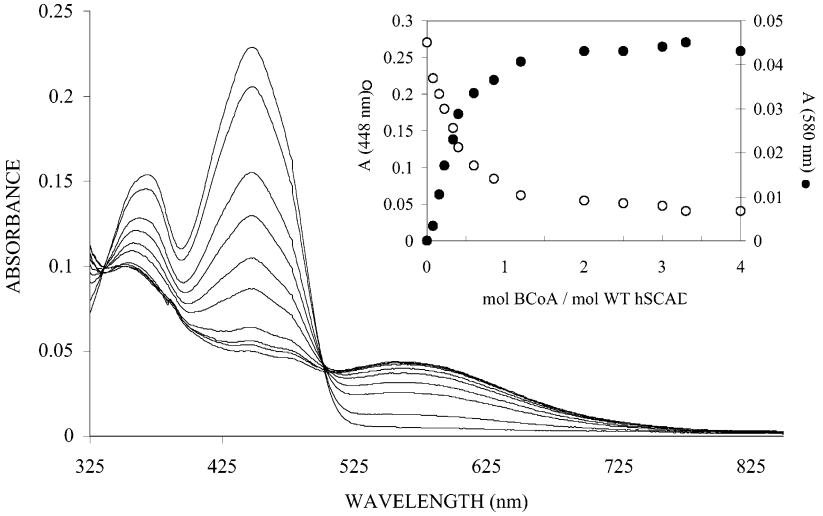

FIGURE 4: Anaerobic substrate titration of wild-type hSCAD (12.4 μM) with butyryl-CoA. Titrations were performed at 25 °C in 50 mM potassium phosphate buffer (pH 7.6) with 100 μM methyl viologen. Curves 1−10: [butyryl-CoA] = 0.0, 1.3, 13.2, 15.8, 18.4, 21.0, 23.6, 26.2, 28.8, and 33.9 μM, respectively. Inset: Plot of absorbance at 448 nm (○) and 580 nm (●) as a function of substrate added.

The $\Delta\hat{E}$ values determined for wild-type hSCAD titrations with butyryl-, valeryl-, and hexanoyl-CoA were −21, −15, and −10 mV, respectively, calculated after spectral examination of each titration. These values indicate that the potential of the enzyme-bound substrate/product couple is more negative than the flavin, i.e., electron transfer from substrate to the FAD cofactor is now highly favored. These shifts are pictorially represented in Figure 3 (solid bars). There is the most thermodynamic overlap between hSCAD and BCoA/CCoA, indicating that this thioester couple has the greatest ability to activate acyl-CoA substrates and 2-enoyl-CoA products. The $\Delta\hat{E}$ values become slightly less with increasing chain length. However, the overall potential achieved by each enzyme-bound substrate/product couple is remarkably similar (ca. −73 mV). Because hSCAD has optimal activity with butyryl-CoA, these results are consistent with the idea that increased enzyme activity with a ligand increases the amount of thermodynamic modulation. The potential shifts observed in the hSCAD system with BCoA are the largest observed in any acyl-CoA dehydrogenase system studied, indicating that both the enzyme *and* the substrate/product couple requires significant amounts of modulation for electron transfer to occur. It is of considerable interest to subsequently determine how mutations responsible for SCAD deficiency in humans affect the redox potentials of the free enzyme and the substrate/product couple.

Electrochemical Characterization of Kinetically Dead Mutants. The results obtained with wild-type hSCAD are enhanced through studies with the kinetically dead E368Q mutant enzyme. A coulometric titration was initially performed on this mutant. Calculations from this titration experiment revealed a two-electron transfer with little blue and no red semiquinone stabilized. This trend was also previously observed with the E367Q bSCAD mutant in earlier studies (*8*). The visible spectra of the wild-type and E368Q mutant hSCAD were similar during coulometric reduction except for a slight red shift and slightly higher resolution of the flavin maximum (452 versus 448 nm).

Table 2 reports the electrochemical and binding data obtained for E368Q hSCAD. The $E_{ox/hq}$ potential for the uncomplexed E368Q hSCAD mutant is −141 mV, a value that is 21 mV more positive than wild-type hSCAD. Similar shifts were seen in a human MCAD E376Q catalytic base mutant, which demonstrated a positive shift of 33 mV compared to recombinant wild-type MCAD (*19*). The positive shifts observed upon mutation of the glutamate residues to a glutamine is likely due to the removal of a negative charge around the environment of the active sites, thus increasing the hydrophobicity. Midpoint potentials of the FAD active sites have been shown to be sensitive to charged groups in the protein environment (*19*, *26*). The individual formal potential values of $E_1^{\circ\prime}$ and $E_2^{\circ\prime}$ are separated by similar amounts in this protein as no red or blue semiquinone formation during the course of the potentiometric titrations is observed.

Table 2: Dissociation Constants and Midpoint Potentials[a] for Uncomplexed and Ligand Complexed E368Q hSCAD

ligand	K_{dox} (μM)	$E_{ox/hq}$ (mV)[b]	$\Delta E_{ox/hq}$ (mV)	% Sq[c]
none		−141	0	≤5
butyryl-CoA	1.34	−103	+38	≤5
crotonyl-CoA	1.7	−110	+31	≤5
valeryl-CoA	1.9	−116	+25	≤5
pentenoyl-CoA	1.41	−103	+38	≤5
hexanoyl-CoA	4.38	−137	+4	≤5
hexenoyl-CoA	2.88	−108	+33	≤5
octanoyl-CoA	125.3	−161	−20	≤5
octenoyl-CoA	21.3	−118	+23	≤5

[a] Potentials and dissociation constants recorded at 25 °C in 50 mM potassium phosphate buffer, pH 7.6. [b] All midpoint potential determinations were calculated from an average of three trials with a typical error of ± 2−5 mV. [c] Maximum percentage of enzyme stabilized in blue neutral semiquinone form during potentiometric titration of uncomplexed or complexed enzyme.

The midpoint potential for the E367Q bSCAD mutant was also performed to allow comparison with potentials determined when the enzyme is ligand bound. Table 3 presents the data obtained with this mutant. A reduction potential value of −66 mV was calculated, a value that is within experimental error of the previously reported value (*8*). This is 13 mV more positive than the reduction potential value for recombinant wild-type bSCAD (−79 mV), again consistent with the earlier hypothesis that removing the negative charge increases the hydrophobicity of the active site.

Table 3: Dissociation Constants and Midpoint Potentials[a] for Uncomplexed and Ligand Complexed E367Q bSCAD

ligand	K_{dox} (μM)	$E_{ox/hq}$ (mV)[b]	E_1	E_2	$\Delta E_{ox/hq}$ (mV)	% Sq[c]
none		−66[d]	−123	−5	0	≤5
butyryl-CoA	6.2	−73	−72	−73	−7	34[d]
crotonyl-CoA	2.2	−34	−31	−37	+32	36[d]
valeryl-CoA	5.8	−71			−5	≤5
pentenoyl-CoA	4.59	−44			+22	≤5
hexanoyl-CoA	4.77	−60			+6	≤5
hexenoyl-CoA	4.01	−50			+16	≤5

[a] Potentials and dissociation constants recorded at 25 °C in 100 mM potassium phosphate buffer, pH 7.0. [b] All midpoint potential determinations were calculated from an average of three trials with a typical error of ± 2−5 mV. [c] Maximum percentage of enzyme stabilized in blue neutral semiquinone form during potentiometric titration of uncomplexed or complexed enzyme. [d] From ref *8*.

Coulometric enzyme reduction also reveals a two-electron transfer, less than 6% blue neutral semiquinone, and no red anionic semiquinone stabilization. This observation is also in agreement with previous experimental data (*8*).

Determination of Binding Constants for E368Q hSCAD and E367Q bSCAD. The effects of substrate and product binding to the kinetically dead mutants E368Q hSCAD and E367Q bSCAD were examined. Because these mutants are incapable of enzyme turnover, the binding effects of each ligand (substrate and product) could be determined separately. The ligands used with E368Q hSCAD were butyryl-, crotonyl-, valeryl-, pentenoyl-, hexanoyl-, hexenoyl-, octanoyl-, and octenoyl-CoA. Studies with E367Q bSCAD utilized all of the above ligands except for octanoyl- and octenoyl-CoA.

Free E368Q has a calculated extinction coefficient of 14.3 mM^{-1} cm^{-1}, and uncomplexed E367Q has a slightly lower extinction coefficient of 13.9 mM^{-1} cm^{-1}. Upon addition of substrate, spectral changes that are typical of those associated with ACD active site desolvation occur as changes occur near the isoalloxazine ring of the flavin (*27*), and the flavin absorbance becomes red-shifted, more well-resolved, and slightly quenched. No hydratase activity toward any ligand is observed in either the E368Q hSCAD or the E367Q bSCAD systems. This was determined by lack of a CT band after incubation of a ligand after 20 h at 25 °C. The extinction coefficients calculated for each inactive mutant bound to a ligand are shown in Table 1. The extinction coefficients are all similar, except that the E367Q bSCAD mutants have lower extinction coefficients when ligand bound than the E368Q mutants.

A K_{dox} was calculated for each ligand by following the absorbance changes at 485 nm (or each λ_{max} as determined by subtraction of the uncomplexed from the complexed spectrum) as a function of the ligand concentration. A typical binding experiment is shown in Figure 5 and the binding spectra were similar for E368Q hSCAD and E367Q bSCAD. The values for the binding constants for E368Q hSCAD are presented in Table 2, and the binding constants for the E367Q bSCAD system are shown in Table 3. All SCAD systems have an optimal specificity for substrates with a carbon chain length of four to six carbons. In the E368Q hSCAD system similar binding constants were calculated for both the substrates and the products with carbon chain lengths of four and five carbons. The hexanoyl- and hexenoyl-CoA substrate and product showed slightly less favorable binding to the enzyme, with the product binding more tightly than the substrate by a factor of 1.5. In addition, the C8 ligands did not bind as tightly to the enzyme compared to other ligands, especially octanoyl-CoA. This is likely due to the ligand not fitting properly into the active site of the enzyme because of increased steric properties. Similar binding effects in SCAD were observed in studies utilizing longer chain length ligands (*7*). Binding of the eight-carbon chain length ligands also resulted in less prominent shoulders and less flavin bleaching, probably an effect of the active site being only partially desolvated.

E367Q bSCAD exhibited an opposite trend with respect to the optimal chain length substrate and product. In E368Q hSCAD, the substrate (butyryl-CoA) bound more tightly to the enzyme, while in E367Q bSCAD the product (crotonyl-CoA) was bound more tightly. In addition, bSCAD showed tighter binding to all of the products compared to the substrates. This finding could be because bSCAD in its natural environment uses product to catalyze its electron-transfer reaction. Studies of C8 bound ligands to E367Q bSCAD were not conducted due to the less than optimal binding observed with E368Q hSCAD.

Electrochemical Studies of E368Q/Ligand Complexes. Coulometric titrations of the ligand saturated E368Q complexes were used to determine the oxidation state of the ligand throughout the titration, as well as to ensure no co-reduction would take place during the course of the potentiometric experiments. All of the coulometric experiments performed with ligand saturated E368Q yielded a value for $n \approx 2.0 \pm 0.3$, suggesting that no enzyme turnover was occurring and that each ligand/enzyme pair would be suitable for midpoint potential determination. Following the absorbance of the flavin at 450 nm allowed the oxidation state of the enzyme to be identified. None of the ligand/enzyme complexes demonstrated more than minimal (<5%) semiquinone stabilization throughout the course of the experiments.

Upon the basis of the previously determined K_{dox} for each ligand complexed to each enzyme, ligand saturated enzyme solutions were created and studied spectroelectrochemically. The redox state of the enzyme was determined after each sequential addition of reducing equivalents by monitoring the absorbance at 450 nm. A typical experiment is shown in Figure 6 and the average midpoint potentials for the ligand saturated E368Q, as well as the $\Delta E_{ox/hq}$, are presented in Table 2. The reactions all proceed as a two-electron transfer, as indicated by the Nernstian slope, and semiquinone amounts stabilized were all minimal, although large amounts of CT bands were observed.

An interesting trend appears upon examination of the $\Delta E_{ox/hq}$ values for substrate and product bound E368Q hSCAD. The optimal substrate (butyryl-CoA) shifts the midpoint potential of the enzyme more positive (+ 38 mV) than optimal product (crotonyl-CoA) does (+ 31 mV), which is the opposite shift induced in the analogous bSCAD enzyme. This is complementary to studies performed with wild-type hSCAD, in which substrate produces large degrees of thermodynamic modulation in the protein, and concurs with the binding data presented.

In the longest chain length substrate studied (octanoyl-CoA), the flavin redox potential actually shifted more

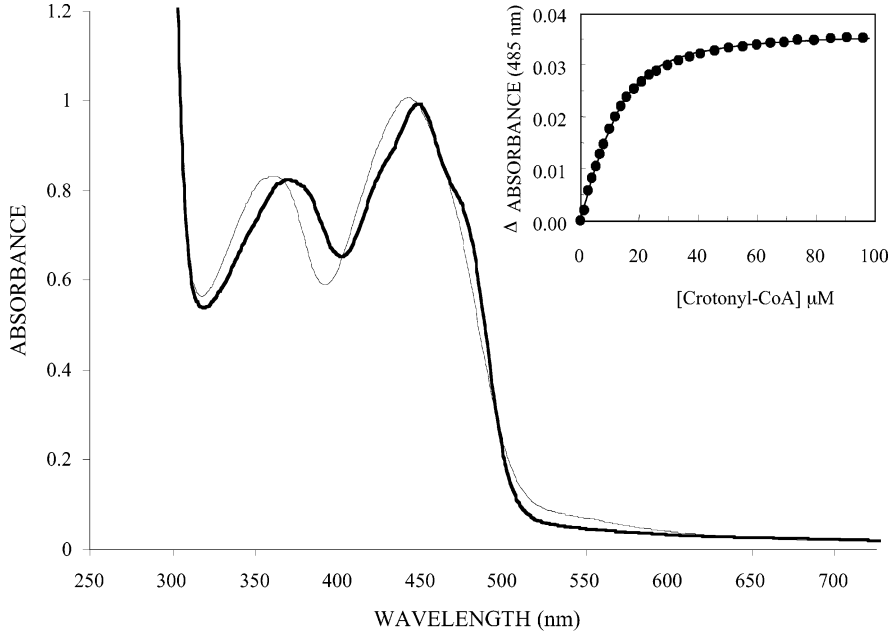

FIGURE 5: Typical ligand binding to E368Q hSCAD; binding titration shown is E368Q hSCAD binding to crotonyl-CoA. The thin black line represents free enzyme, while the thick black line depicts ligand-saturated enzyme. Spectra were recorded in 50 mM potassium phosphate buffer, pH 7.6 for E368Q hSCAD and 100 mM potassium phosphate buffer, pH 7.0 for E367Q bSCAD at 25 °C. Inset: Plot of change in absorbance at 485 nm upon titration of E368Q hSCAD with crotonyl-CoA (●). These data were fit to a K_{dox} of 1.8 ± 0.12 μM (—).

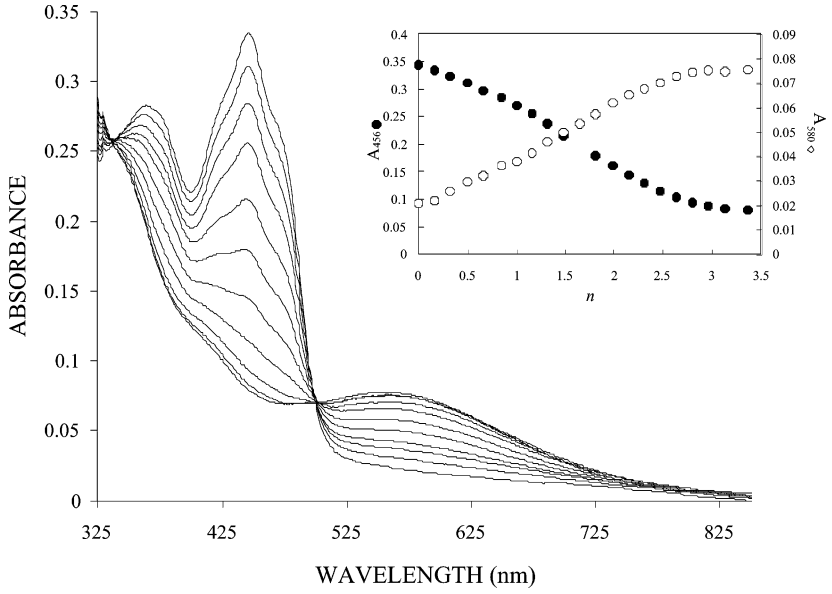

FIGURE 6: Coulometric titration of hexenoyl-CoA saturated E368Q hSCAD (14.1 μM) in 50 mM potassium phosphate buffer (pH 7.6). Titration was performed at 25 °C under anaerobic conditions using methyl viologen (100 μM) as the mediator dye. Selected spectra are shown for clarity. Inset: Relationship between the number of reducing equivalents and the absorbances at 456 nm (protein) and 580 nm (charge-transfer).

negative, thus creating a more unfavorable environment for electron transfer. These findings, taken together with the binding data, suggest that the substrate is not properly aligned within the active site and may only be partially desolvating the active site. Similar findings were observed using pyrrolic analogues with bSCAD (*7*). Nonoptimal binding combined with negative potential shifts suggests that the ligand may be binding to another site of the enzyme, likely another flavoprotein (electron transferring flavoprotein) binding site.

Interestingly, the products produced larger flavin potential shifts than the substrates in the subsequent studies in E368Q hSCAD. Recall that products also bound more tightly than substrates (with the exception of crotonyl-CoA). Although the shifts produced individually by each substrate and product in the E368Q mutant protein are not as large as that induced by the substrate/product couple on the wild-type enzyme, taken together they yield a representative picture of how each ligand affects the binding and electrochemical properties of the enzyme. Desolvation of the active site and ligand polarization have both been shown through electrochemical studies utilizing product analogues to contribute to flavin potential shifts induced by ligand binding (*21*, *28*). Resonance Raman and NMR studies performed by Nishina and co-workers have provided additional insight into enzyme activation by product binding (*24*, *29*, *30*). One of their key discoveries was that the electronic structure of natural product

in MCAD, *trans*-2-octenoyl-CoA, has appreciable contribution from an enolate resonance form in the presence of reduced enzyme. In the bSCAD system, product formation was found more favorable in systems that had greater $\pi-\sigma$ interactions with the flavin isoalloxazine ring, suggesting that electrostatic environment around the flavin plays a role in substrate/product activation (*20*). It is likely that product binding in hSCAD also contributes largely to the observed potential shifts; however, in this system the *role that natural substrate plays* in enzyme activation now cannot be discounted.

Electrochemical Studies of E367Q/Ligand Complexes. Finally, identical electrochemical experiments were conducted with the E367Q bSCAD/ligand complexes to allow comparison between two different short-chain ACD systems. The midpoint potentials, potential shifts, and amounts of thermodynamically stabilized semiquinone are presented in Table 3. Each thioester product shifted the flavin midpoint potential to larger degrees than the substrate did, with crotonyl-CoA producing the largest shift and hexenoyl-CoA the smallest. In contrast, both the C4 and the C5 substrates shifted the potential negative, and the shift induced by the C6 substrate was minimal. Large amounts of semiquinone were also observed throughout the reductive titrations of bSCAD with natural substrate and product, but only CT bands were observed in experiments utilizing the nonoptimal thioesters. Again, it can be noted that the product bound more tightly than the substrate, and thus larger potential shifts were produced. These observations and trends support the overall findings that in the bSCAD enzyme product has larger contributions to enzyme activation than does substrate.

CONCLUSION

Our results indicate an overall high degree of thermodynamic modulation of wild-type hSCAD. This enzyme exhibits a highly tuned system with levels of substrate activation that have not previously been reported with other acyl-CoA dehydrogenases. Electrochemical studies indicate that natural substrates of varying chain lengths induce large potential shifts (33 mV) of the actual substrate/product couple, an interesting phenomenon that proves to be a necessity for electron transfer to occur from the fatty acyl-CoA to the flavin cofactor. Further insight into regulation of hSCAD is gained from the kinetically dead mutant, E368Q. Binding of butyryl-CoA and the potential shifts associated with this binding support the findings with wild-type enzyme. Although the hSCAD and bSCAD enzymes catalyze the same reaction and are structurally very similar, hSCAD clearly demonstrates a greater need for substrate activation than does bSCAD.

Although the crystal structure for human SCAD has not been completed, comparisons can be made between the structures of rat SCAD, which shares similar sequence and homology to human SCAD, and bacterial SCAD. A careful comparison between rat and bacterial SCAD showed no significant differences between the substrate binding sites of the two enzymes (*31*). Thus, the differences in the redox properties between human and bacterial SCAD are likely caused by more subtle interactions. The proposed mechanism of these enzymes begins with a enzyme/substrate complex, followed by an isomerization step, and ending with electron transfer. The nature of the isomerization reaction is still unclear and currently under investigation. A more thorough understanding of the isomerization step will be necessary to fully comprehend the redox shifts and differences experimentally observed between the two enzymes.

The binding of various natural thioester ligands to the kinetically dead forms of each enzyme induces different shifts in the redox properties. The greatest similarity between the two systems was that product produces greater overall redox potential shifts (with the exception of crotonyl-CoA); thus, it is postulated that the product/enzyme complex more closely resembles the transition state complex than the substrate/enzyme complex. Ultimately, it will be possible to gain more insight into this process by examining the consequences of failed substrate activation and the effect on the spectral and electrochemical properties of the enzyme.

REFERENCES

1. Sherratt, H. S. A. (1988) The enzymology of beta-oxidation. Introductory remarks, *Bio. Chem. Soc. Trans. 16*, 409.
2. Lenn, N. D., Stankovich, M. T., and Liu, H. (1990) Regulation of the redox potential of general acyl-CoA dehydrogenase by substrate binding, *Biochemistry 29*, 3709−3715.
3. Djordjevic, S., Pace, C. P., Stankovich, M. T., and Kim, J.-J. (1995) Three-dimensional structure of butyryl-CoA dehydrogenase from Megasphaera elsdenii, *Biochemistry 34*, 2163−2171.
4. Vock, P., Engst, S., Elder, M., and Ghisla, S. (1998) Substrate activation by acyl-CoA dehydrogenases: transition-state stabilization and pKs of involved functional groups, *Biochemistry 37*, 1848−1860.
5. Rudik, I., Ghisla, S., and Thorpe, C. (1998) Protonic equilibria in the reductive half-reaction of the medium-chain acyl-CoA dehydrogenase, *Biochemistry 37*, 8437−8445.
6. Stankovich, M. T., and Soltysik, S. (1987) Regulation of the butyryl-CoA dehydrogenase by substrate and product binding, *Biochemistry 26*, 2627−2632.
7. Lamm, T. R., Kohls, T., Saenger, A. K., and Stankovich, M. T. (2003) Comparison of ligand polarization and enzyme activation in medium- and short-chain acyl-coenzyme A dehydrogenase-novel analog complexes, *Arch. Biochem. Biophys. 409*, 251−261.
8. Becker, D. F., Fuchs, J. A., and Stankovich, M. T. (1994) Product binding modulates the thermodynamic properties of a Megasphaera elsdenii short-chain acyl-CoA dehydrogenase active-site mutant, *Biochemistry 33*, 7802−7807.
9. Nguyen, T. V., Riggs, C., Babovic-Vuksanovic, D., Kim, Y.-S., Carpenter, J. F., Burghardt, T. P., Gregersen, N., and Vockley, J. (2002) Purification and characterization of two polymorphic variants of short chain acyl-CoA dehydrogenase reveal reduction of catalytic activity and stability of the Gly185Ser enzyme, *Biochemistry 41*, 11126−11133.
10. Williamson, G., and Engel, P. C. (1982) A convenient and rapid method for the complete removal of CoA from butyryl-CoA dehydrogenase, *Biochim. Biophys. Acta 706*, 245−248.
11. Becker, D. F., Fuchs, J. A., Banfield, D. K., and Stankovich, M. T. (1993) Characterization of wild-type and an active-site mutant in *Escherichia coli* of short-chain acyl-CoA dehydrogenase from Megasphaera elsdenii, *Biochemistry 32*, 10736−10742.
12. Lehman, T. C., Hale, D. E., Bhala, A., and Thorpe, C. (1990) An acyl-coenzyme A dehydrogenase assay utilizing the ferricenium ion, *Biochemistry 186*, 280−284.
13. Bernert, J. T., Jr., and Sprecher, H. (1977) An analysis of partial reactions in the overall chain elongation of saturated and unsaturated fatty acids by rat liver microsomes, *J. Biol. Chem. 252*, 6737−6744.
14. Stadtman, E. R. (1957) Preparation and assay of acyl-coenzyme A and other thiol esters; use of hydroxylamine, *Methods Enzymol. 3*, 931−941.
15. Stankovich, M. T. (1980) An anaerobic spectroelectrochemical cell for studying the spectral and redox properties of flavoproteins, *Anal. Biochem. 109*, 295−308.

16. Johnson, B. D., and Stankovich, M. T. (1993) Influence of two substrate analogues on thermodynamic properties of medium-chain acyl-CoA dehydrogenase, *Biochemistry 32*, 10779−10785.
17. Clark, W. M. (1960) in *Oxidation−Reduction Potentials of Organic Systems*, Williams and Wilkins, New York.
18. Johnson, B. D., Mancini-Samuelson, G. J., and Stankovich, M. T. (1995) Effect of transition-state analogues on the redox properties of medium-chain acyl-CoA dehydrogenase, *Biochemistry 34*, 7047−7055.
19. Mancini-Samuelson, G. J. (1996), Ph.D. Thesis, Department of Chemistry, University of Minnesota, Minneapolis.
20. Pellett, J. D., Becker, D. F., Saenger, A. K., Fuchs, J. A., and Stankovich, M. T. (2001) Role of aromatic stacking interactions in the modulation of the two-electron reduction potentials of flavin and substrate/product in Megasphaera elsdenii short-chain acyl-coenzyme A dehydrogenase, *Biochemistry 40*, 7720−7728.
21. Pellett, J. D., Sabaj, K. M., Stephens, A. W., Bell, A. F., Wu, J., Tonge, P. J., and Stankovich, M. T. (2000) Medium-chain acyl-coenzyme A dehydrogenase bound to a product analogue, hexadienoyl-coenzyme A: effects on reduction potential, pK(a), and polarization, *Biochemistry 39*, 13982−13992.
22. Schopfer, L. M., Massey, V., Ghisla, S., and Thorpe, C. (1988) Oxidation−reduction of general acyl-CoA dehydrogenase by the butyryl-CoA/crotonyl-CoA couple. A new investigation of the rapid reaction kinetics, *Biochemistry 27*, 6599−6611.
23. Engel, P. C., and Massey, V. (1971) Green butyryl-coenzyme A dehydrogenase. An enzyme-acyl-coenzyme A complex, *Biochem. J. 125*, 889−902.
24. Nishina, Y., Sato, K., Hazekawa, I., and Shiga, K. (1995) Structural modulation of 2-enoyl-CoA bound to reduced acyl-CoA dehydrogenases: a resonance Raman study of a catalytic intermediate, *J. Biochem. 117*, 800−808.
25. Thorpe, C., Matthews, R. G., and Williams, C. H. (1979) Acyl-coenzyme A dehydrogenase from pig kidney. Purification and properties, *Biochemistry 18*, 331−337.
26. Pellett, J. D. (2000) Ph.D. Thesis, Department of Chemistry, University of Minnesota, Minneapolis.
27. Powell, P. J., Lau, S. M., Killian, D., and Thorpe, C. (1987) Interaction of acyl coenzyme A substrates and analogues with pig kidney medium-chain acyl-coA dehydrogenase, *Biochemistry 26*, 3704−3710.
28. Stephens, A. W. (2002), Ph.D. Thesis, Department of Chemistry, University of Minnesota, Minneapolis.
29. Tamaoki, H., Nishina, Y., Shiga, K., and Miura, R. (1999) Mechanism for the recognition and activation of substrate in medium-chain acyl-CoA dehydrogenase, *J. Biochem. 125*, 285−296.
30. Nishina, Y., Sato, K., Shiga, K., Fujii, S., Kuroda, K., and Miura, R. (1992) Resonance Raman study on complexes of medium-chain acyl-CoA dehydrogenase, *J. Biochem. 111*, 699−706.
31. Battaile, K., Molin-Case, J., Paschke, R., Wang, M., Bennett, D. W., Vockley, J., and Kim, J.-J. (2002) Crystal structure of rat short chain acyl-CoA dehydrogenase complexed with acetoacetyl-CoA: comparison with other acyl-CoA dehydrogenases, *J. Biol. Chem. 277*, 12200−12207.

BI051048Y